Cell Reports, Volume *24*

Supplemental Information

Nuclear Receptor Nur77 Limits the Macrophage Inflammatory Response through Transcriptional Reprogramming of Mitochondrial Metabolism

Duco Steven Koenis, Lejla Medzikovic, Pieter Bas van Loenen, Michel van Weeghel, Stephan Huveneers, Mariska Vos, Ingrid Johanna Evers-van Gogh, Jan Van den Bossche, Dave Speijer, Yongsoo Kim, Lodewyk Wessels, Noam Zelcer, Wilbert Zwart, Eric Kalkhoven, and Carlie Jacoba de Vries

Figure S1

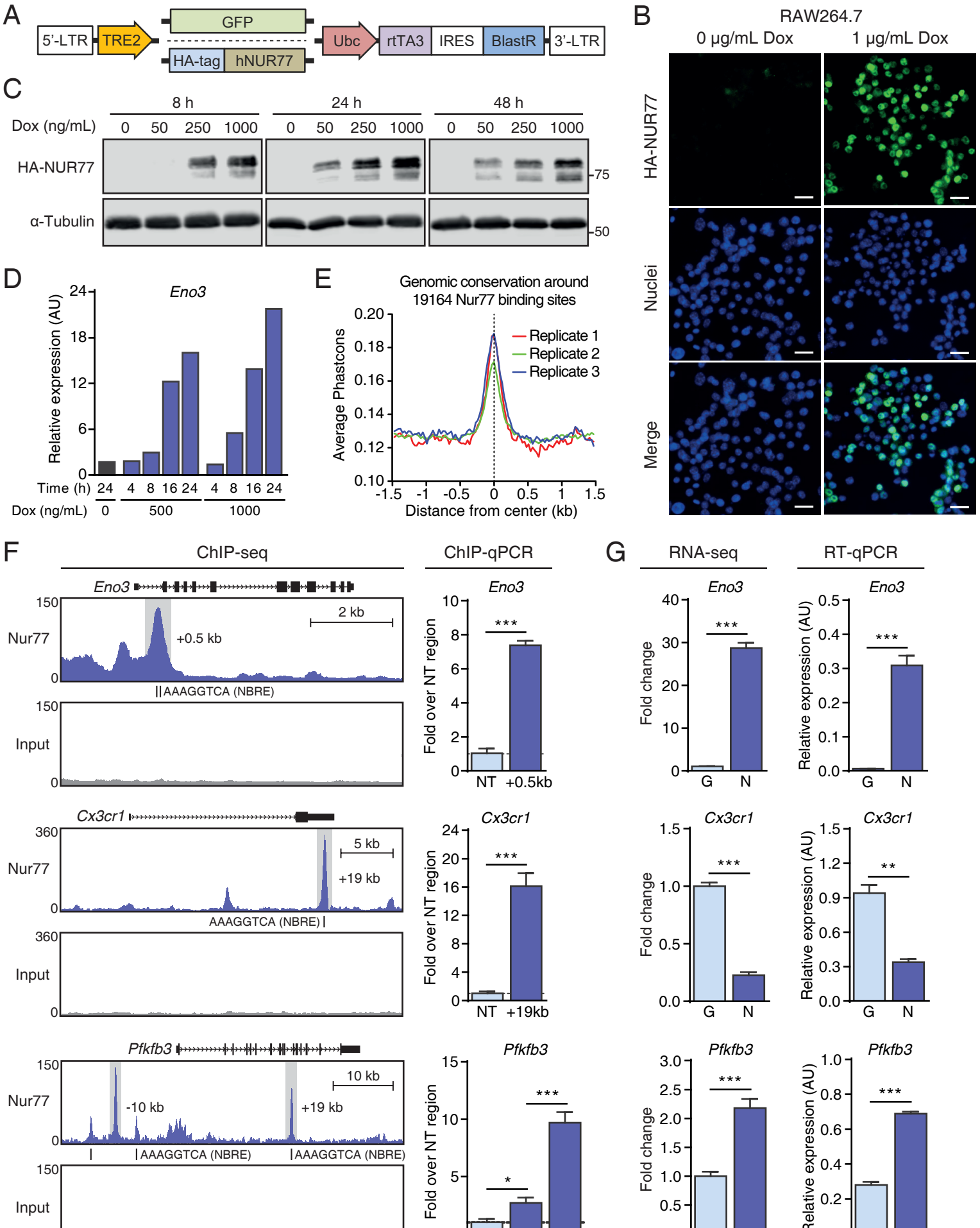
A
5'-LTR
TRE2
GFP
HA-tag
hNUR77
Ubc
rtTA3
IRES
BlastR
3'-LTR
B
RAW264.7
0 µg/mL Dox
1 µg/mL Dox
HA-NUR77
Nuclei
Merge
C
8 h
24 h
48 h
Dox (ng/mL)
0 50 250 1000
HA-NUR77
α-Tubulin
75
50
D
Eno3
Relative expression (AU)
Time (h) 24 4 8 16 24 4 8 16 24
Dox (ng/mL) 0 500 1000
E
Genomic conservation around
19164 Nur77 binding sites
Average Phastcons
Replicate 1
Replicate 2
Replicate 3
Distance from center (kb)
F
ChIP-seq
ChIP-qPCR
Eno3
Nur77
2 kb
+0.5 kb
AAAGGTCA (NBRE)
Input
Fold over NT region
NT +0.5kb
Cx3cr1
5 kb
+19 kb
NT +19kb
Pfkfb3
10 kb
-10 kb
+19 kb
NT -10 +19kb
G
RNA-seq
RT-qPCR
Fold change
Relative expression (AU)
G N

Figure S1. Validation experiments for RAW264.7 stable cell line and Nur77 ChIP-seq and RNA-seq datasets; related to Figure 1.

(A) pINDUCER20b-GFP and pINDUCER20b-HA-NUR77 plasmids used to create RAW264.7 stable cell lines with doxycycline (Dox)-inducible overexpression of green fluorescent protein (GFP) or HA-tagged NUR77 (HA-NUR77).

(B) Immunofluorescence microscopy of HA-NUR77 expression in RAW264.7 stable cell line after 24 h stimulation with 1 µg/mL Dox. Scale bar indicates 20 µm.

(C) Western blot for protein expression of HA-NUR77 in RAW264.7 stable cell line in response to indicated Dox concentrations and incubation times. α-Tubulin was used as loading control. Numbers on the right: molecular weight in kDa.

(D) Gene expression of established Nur77 target gene *Eno3* in response to varying Dox concentrations and incubation times in RAW264.7 stable cell line.

(E) PhastCons placental mammal sequence conservation score for 19164 Nur77 binding sites.

(F) Genome browser view of Nur77 or input control ChIP-seq signal at indicated gene loci. Bar graphs show ChIP-qPCR validation for Nur77 binding in grey shaded areas. For ChIP-qPCR, Nur77 binding at a non-target region (NT; same data used in all 3 graphs) or gene-specific target region after 18 h stimulation with 1 µg/mL Dox was compared. NBRE = Nur77 response element.

(G) Fold change from RNA-seq dataset and RT-qPCR validation for several genes differentially expressed in RNA-seq dataset. Target gene expression after GFP (G) or HA-NUR77 (N) overexpression induced by 18 h stimulation with 1 µg/mL Dox was compared.

For (F-G), data are shown as mean ± SEM (n=3). p-values were calculated using two-tailed Student's t-test. *p<0.05; **p<0.01; ***p<0.001.

Figure S2

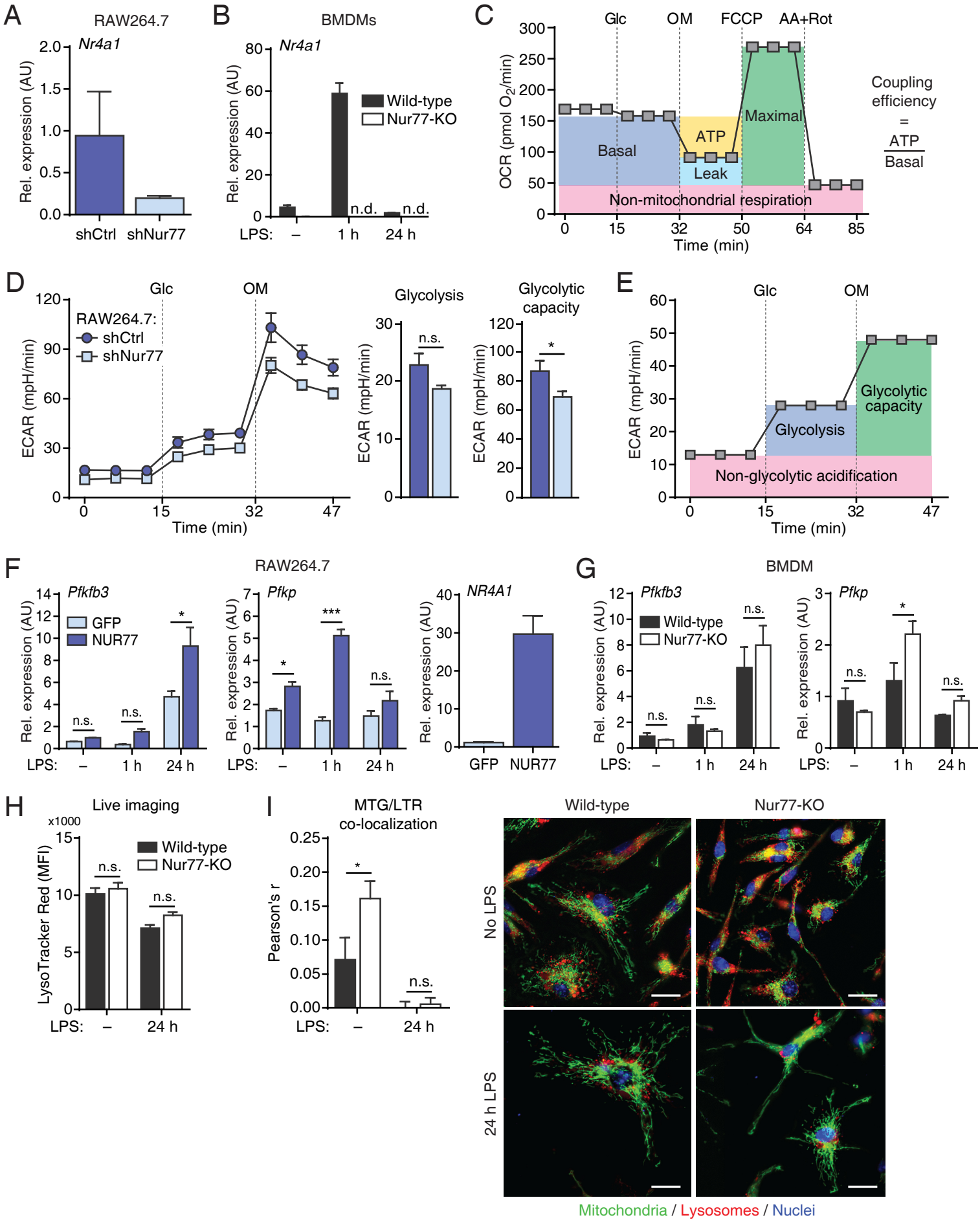
A
RAW264.7
Nr4a1
Rel. expression (AU)
shCtrl
shNur77
B
BMDMs
Nr4a1
Wild-type
Nur77-KO
n.d.
LPS:
1 h
24 h
C
Glc
OM
FCCP
AA+Rot
OCR (pmol O2/min)
Basal
ATP
Leak
Maximal
Non-mitochondrial respiration
Time (min)
Coupling efficiency = ATP / Basal
D
RAW264.7:
shCtrl
shNur77
ECAR (mpH/min)
Glycolysis
Glycolytic capacity
n.s.
E
Glycolysis
Glycolytic capacity
Non-glycolytic acidification
F
RAW264.7
Pfkfb3
Pfkp
NR4A1
GFP
NUR77
G
BMDM
H
Live imaging
LysoTracker Red (MFI)
I
MTG/LTR co-localization
Pearson's r
Wild-type
Nur77-KO
No LPS
24 h LPS
Mitochondria / Lysosomes / Nuclei

Figure S2. Minor effects of Nur77 on glycolysis in macrophages; related to Figure 2.

(A-B) Gene expression of endogenous Nur77 (*Nr4a1*) after shRNA-mediated knockdown in RAW264.7 (A), or in WT and Nur77-KO BMDMs left untreated or stimulated with LPS for times indicated (B).

(C) Example graph showing OXPHOS parameter calculation from OCR values.

(D) ECAR in RAW264.7 after knockdown of Nur77 (shNur77) versus control (shCtrl) followed by sequential injection of Glc and OM. Bar graphs show parameters of glycolysis derived from ECAR values as illustrated in (E).

(E) Example graph showing glycolytic parameter calculation from ECAR values.

(F-G) Expression of glycolytic genes and exogenous NUR77 in RAW264.7 untreated or stimulated with 500 ng/mL LPS for times indicated while overexpressing GFP or NUR77 (F), or in WT and Nur77-KO BMDMs left untreated or stimulated with LPS for times indicated (G).

(H) Lysosomal abundance in untreated or 24 h LPS-stimulated WT and Nur77-KO BMDMs determined by live-cell imaging of cells stained with LysoTracker Red DND-99. MFI = mean fluorescence intensity.

(I) Co-localization between MitoTracker Green FM (MTG) and LysoTracker Red DND-99 (LTR) in untreated or 24 h LPS-stimulated WT and BMDMs expressed as Pearson's correlation coefficient determined by live-cell imaging of co-stained cells. Micrographs on the right show representative co-stained cells. Scale bar = 20 μm.

For (A-B, D, F-I), data are shown as mean ± SEM (n=3 for A,B,D,F,G; n=35-50 cells for H; n=4 image panels for I). p-values were calculated using two-tailed Student's t-test. *$p<0.05$; **$p<0.01$; ***$p<0.001$.

Figure S3

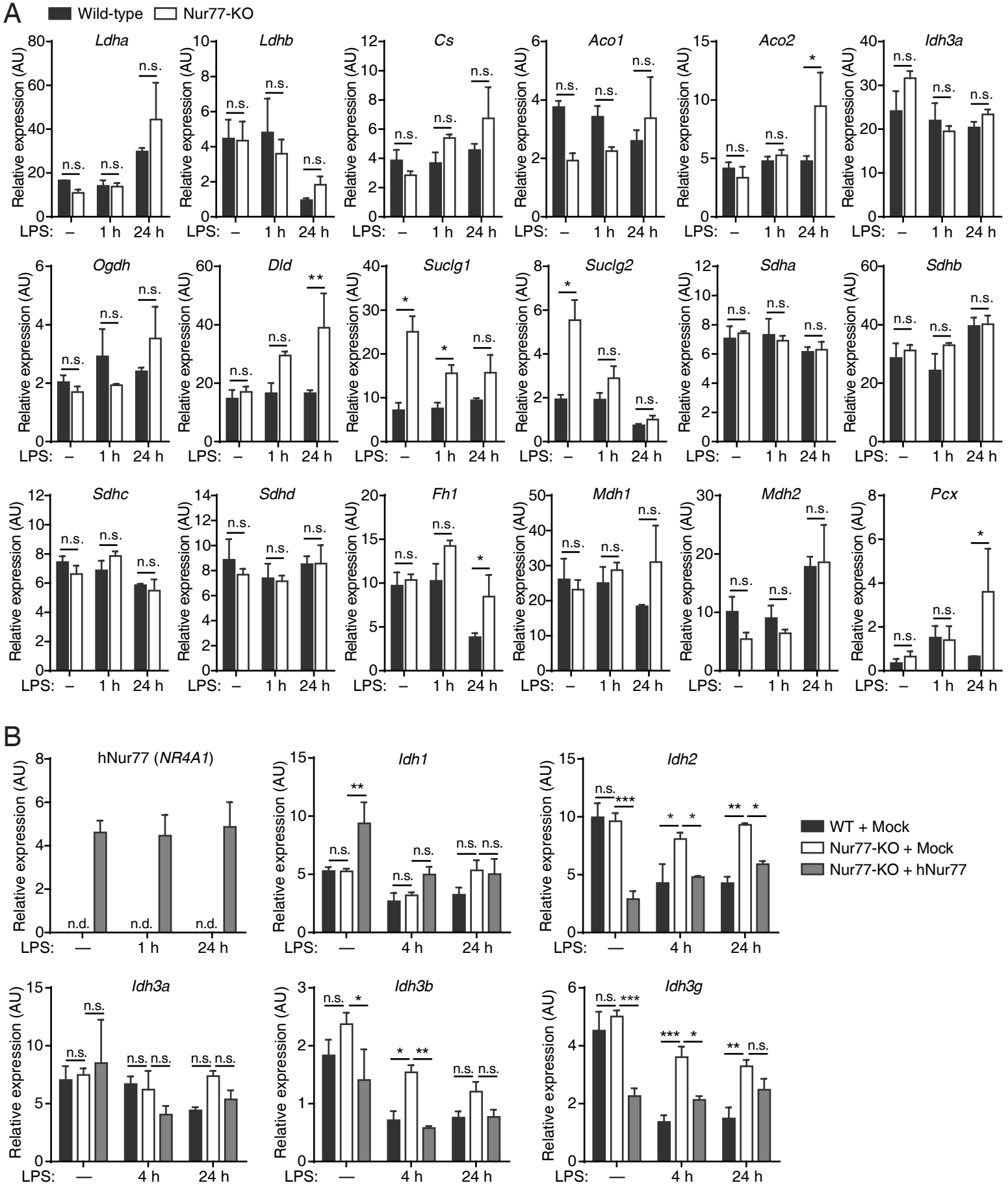
A
Wild-type
Nur77-KO
Ldha
Ldhb
Cs
Aco1
Aco2
Idh3a
Ogdh
Dld
Suclg1
Suclg2
Sdha
Sdhb
Sdhc
Sdhd
Fh1
Mdh1
Mdh2
Pcx
Relative expression (AU)
LPS: – 1 h 24 h
n.s.
*
**
B
hNur77 (NR4A1)
Idh1
Idh2
Idh3a
Idh3b
Idh3g
n.d.
LPS: — 4 h 24 h
WT + Mock
Nur77-KO + Mock
Nur77-KO + hNur77
***

Figure S3. Nur77-deficient macrophages have largely unaltered expression of several TCA cycle enzyme genes, while mitochondrial IDH genes are repressed by Nur77 overexpression; related to Figure 3.

(A) Expression of glycolysis and TCA cycle enzyme genes in WT and Nur77-KO BMDMs left untreated or stimulated with LPS for times indicated.

(B) Expression of human Nur77 (*NR4A1*) and IDH-encoding genes in WT and Nur77-KO BMDMs transduced with human Nur77 (hNur77) or control (Mock) lentivirus and either left untreated or stimulated with LPS for times indicated.

Data are shown as mean ± SEM (n=3). p-values were calculated using two-tailed Student's t-test (A) or two-way ANOVA (B). *p<0.05; **p<0.01; ***p<0.001.

Figure S4

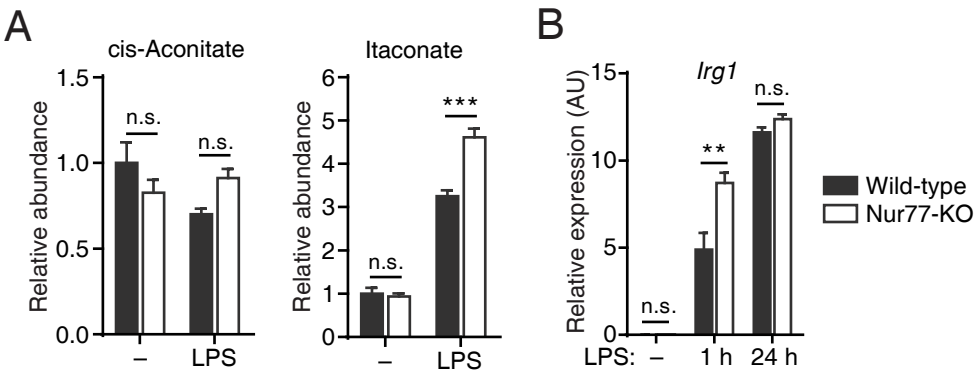

Figure S4. Nur77-deficient macrophages produce more itaconate in response to LPS; related to Figure 4.

(A) Relative abundance of cis-aconitate and itaconate in WT and Nur77-KO BMDMs from metabolomics dataset.

(B) Gene expression of *Irg1* in WT and Nur77-KO BMDMs left untreated or stimulated with LPS for times indicated.

Data are shown as mean ± SEM (n=4-6 for A, n=3 for B). p-values were calculated using two-tailed Student's t test. **p<0.01; ***p<0.001.

Figure S5

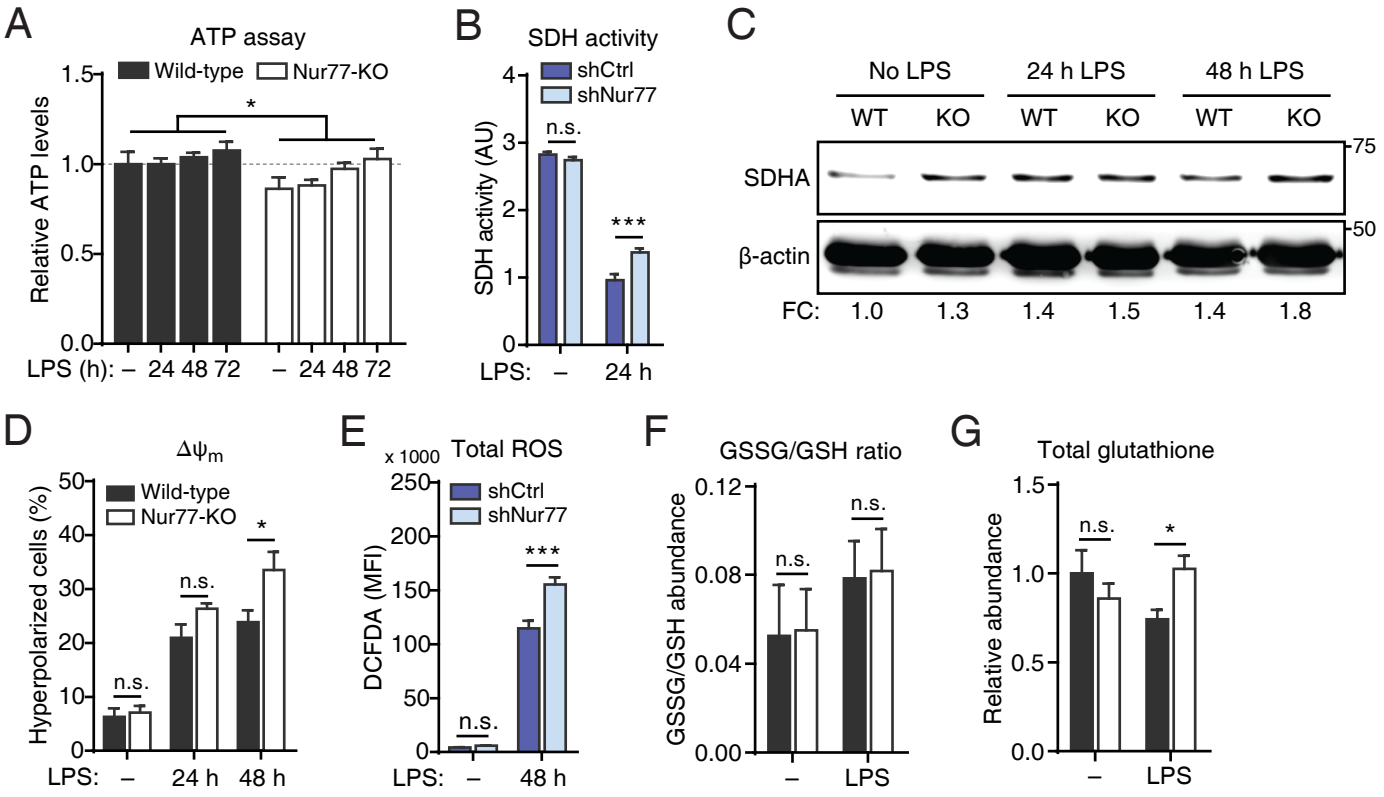

Figure S5. Nur77 deficiency does not alter SDH expression; related to Figure 5.

(A) Relative intracellular ATP levels in WT and Nur77-KO BMDMs left untreated or stimulated with LPS for times indicated. Related to Figure 5B.

(B) SDH activity determined by MTT assay in RAW264.7 after shRNA-mediated knockdown of Nur77 (shNur77) versus control shRNA (shCtrl) and untreated or stimulated with 500 ng/mL LPS for 24 h.

(C) Western blot for SDHA protein in WT and Nur77-KO BMDMs left untreated or stimulated with LPS for times indicated. β-Actin was used as loading control. Numbers on the right: molecular weight in kDa. Numbers at the bottom: FC in β-actin-normalized SDHA band intensity relative to unstimulated WT. Blot shown is representative of three independent experiments.

(D) Quantification of percentage of WT and Nur77-KO BMDMs with hyperpolarized mitochondria after stimulation with LPS for times indicated. Related to Figure 5F.

(E) ROS production determined by flow cytometry in RAW264.7 after knockdown of Nur77 (shNur77) versus control (shCtrl), followed by stimulation with 500 ng/mL LPS for 48 h and staining with DCFDA.

(F-G) Ratio of oxidized (GSSG) to reduced (GSH) glutathione (F) and relative abundance of total glutathione (G) in WT and Nur77-KO BMDMs from metabolomics dataset.

For (A-B, D-G), data are shown as mean ± SEM (n=3 for A, D-E; n=8 for B; n=4-6 for F-G). p-values were calculated using two-tailed Student's t-test (B, D-H) or two-way ANOVA with Tukey post-hoc test (A). *p<0.05; **p<0.01; ***p<0.001.

Figure S6

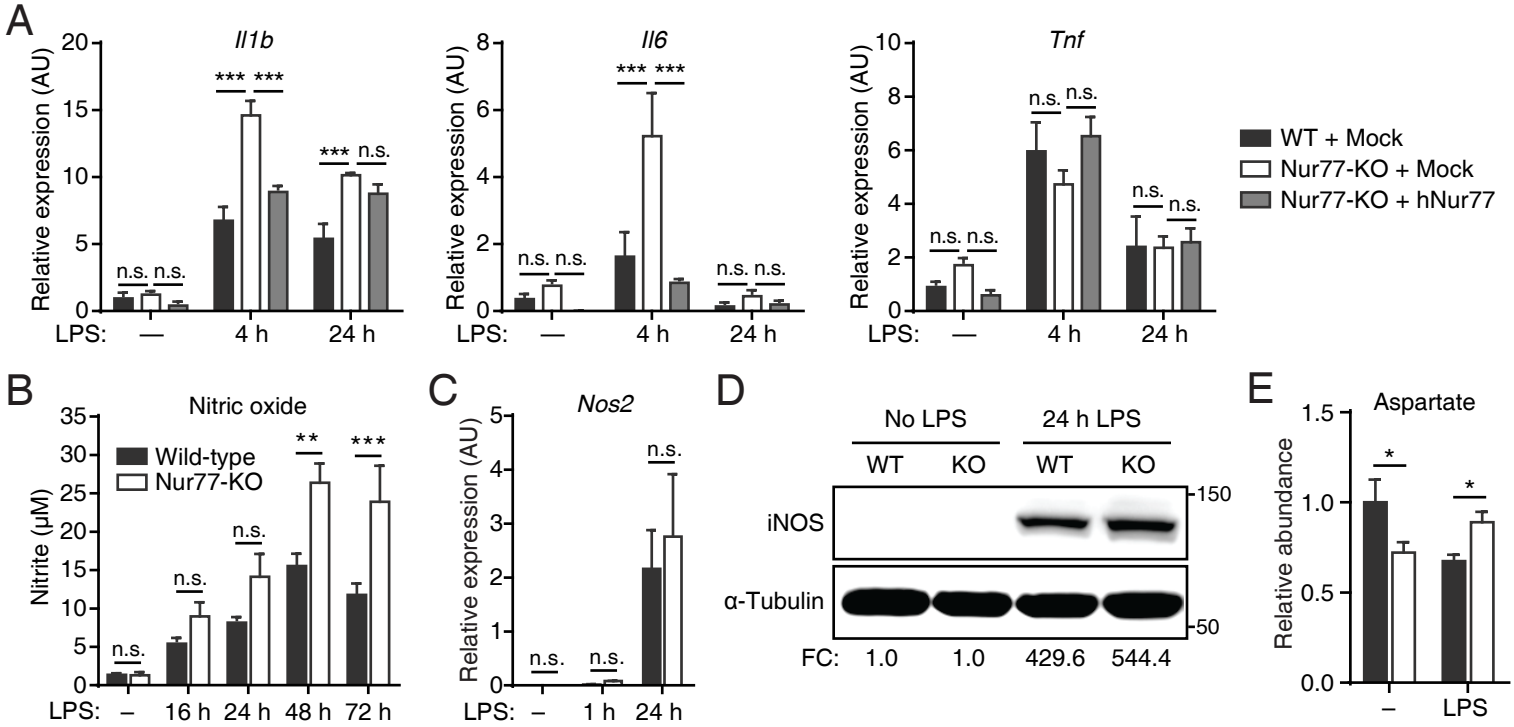

Figure S6. Increased nitric oxide production but unchanged *Nos2* gene and iNOS protein expression in Nur77-KO BMDMs; related to Figure 6.

(A) Cytokine gene expression in WT and Nur77-KO BMDMs transduced with human Nur77 (hNur77) or control (Mock) lentivirus as in Figure S3B and either left untreated or stimulated with LPS for times indicated.

(B-C) NO secretion (B) and *Nos2* gene expression (C) in WT and Nur77-KO BMDMs left untreated or stimulated with LPS for times indicated.

(D) Western blot for iNOS protein in WT and Nur77-KO BMDMs left untreated or stimulated with LPS for 24 h. α-Tubulin was used as loading control. Numbers on the right: molecular weight in kDa. Numbers at the bottom: FC in α-Tubulin-normalized iNOS band intensity relative to unstimulated WT. Blot shown is representative of two independent experiments.

(E) Relative abundance of aspartate in WT and Nur77-KO BMDMs from metabolomics dataset.

For (A-C, E), data are shown as mean ± SEM (n=3 for A-C; n=4-6 for E). p-values were calculated using two-way ANOVA with Tukey post-hoc test. *p<0.05; **p<0.01; ***p<0.001.

Figure S7

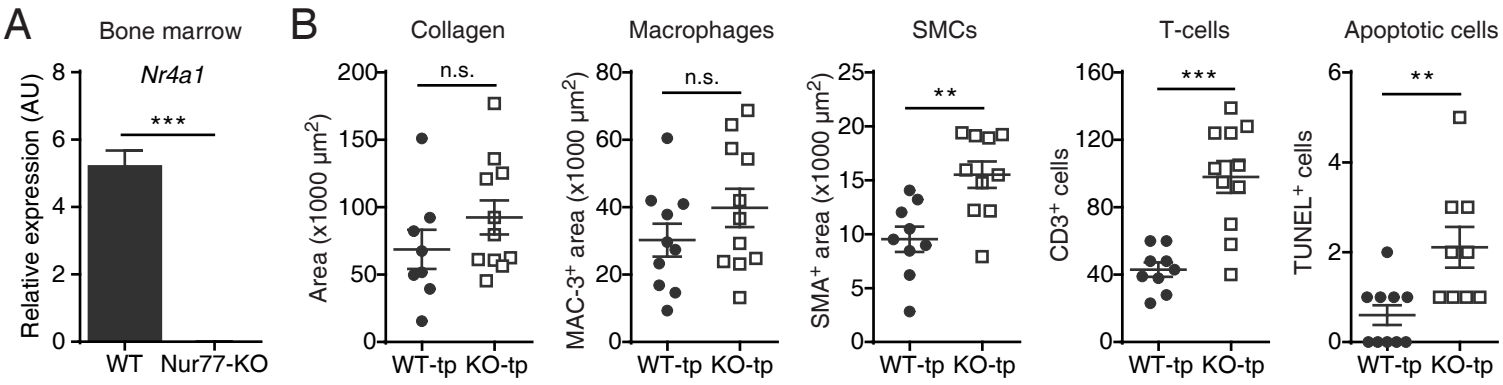

Figure S7. Bone marrow Nur77 deficiency leads to increased numbers of SMCs, T-cells, and apoptotic cells, but unchanged collagen or macrophage content in atherosclerotic lesions; related to Figure 7.

(A) Mouse Nur77 (*Nr4a1*) gene expression in bone marrow cells harvested from WT and Nur77-KO mice.

(B) Characterization of atherosclerotic lesions from WT-tp and KO-tp mice described in Figure 7A, showing quantification of collagen deposition and macrophage (MAC-3$^+$), smooth muscle cell (SMC; SMA$^+$), T-cell (CD3$^+$), and apoptotic cell (TUNEL$^+$) content in each lesion.

For (B), each filled circle (WT-tp) or hollow square (KO-tp) indicates one mouse and horizontal bars indicate mean ± SEM. p-values were calculated using two-tailed Student's t test. *p<0.05; **p<0.01; ***p<0.001.